

# Strained-layer growth and islanding of germanium on Si(111)-(7 × 7) studied with STM

U. Köhler, O. Jusko, G. Pietsch, B. Müller<sup>1</sup> and M. Henzler

*Institut für Festkörperphysik, Universität Hannover, Appelstrasse 2, W-3000 Hannover, Germany*

Received 17 August 1990; accepted for publication 12 December 1990

The growth of in situ prepared germanium layers on Si(111)-(7 × 7) has been studied as a function of substrate temperature and coverage. At room temperature, Ge grows in irregular clusters arranged in an ordered array on the substrate and the (7 × 7) reconstruction is preserved. At elevated temperature, in the submonolayer range triangular islands form with preferred growth in  $[\bar{1}\bar{1}2]$  direction. The islands show Si-like (7 × 7) and (5 × 5) DAS reconstruction. Ge nucleates preferentially at step edges and at (7 × 7) domain boundaries. Coverages over 2 ML result in a completely (5 × 5) reconstructed layer. On substrate with a  $(\sqrt{3} \times \sqrt{3})R30^\circ$  adatom arrangement after boron segregation, the Ge epilayer also exhibits DAS reconstructions of the same kind found on the pure Si substrates. Above 4 ML the formation of 3D islands is observed, which show mainly (113) and (111) facets. The islands are relaxed and show a mixture of  $c(2 \times 8)$ ,  $c(2 \times 4)$ , and (2 × 2) reconstructions known for bulk Ge(111), when they are grown below 450 °C. At a higher deposition temperature a (7 × 7) reappears on top of the 3D islands. Defects emerging from the bulk have been imaged.

## 1. Introduction

The MBE growth of germanium on silicon has attracted considerable interest in the last few years, both from the technological point of view as well as a model system for strained-layer growth. While this topic has been discussed controversially in the past, today there is general agreement in the literature that germanium grows in a Stranski–Krastanov mode (SK mode) on silicon [1]. For the first 4 or 5 monolayers (ML), Ge forms a pseudomorphic layer which is compressed to match the Si lattice; excess germanium at higher coverages piles up in three-dimensional islands. Especially for the very low coverage regime, no detailed information exists of the nucleation behaviour and the atomic arrangement of the epilayer. The goal of our investigation was to study the morphology of the Ge layers starting from the submonolayer range to the regime where 3D islanding occurs.

## 2. Experimental

The experiments were carried out in an UHV chamber (base pressure:  $1 \times 10^{-10}$  mbar) containing the STM, LEED, CMA-Auger spectrometer, and different evaporation sources. Through a load-lock samples and STM tips can be transferred without breaking the UHV. The STM uses a lever-type mechanism for coarse sample–tip approach similar to the one described ref. [2]. As substrates we used  $0.01 \Omega \cdot \text{cm}$  Si(111) wafers with a random miscut < 0.2%. The surfaces were cleaned in situ by thermally removing the native oxide at 920 °C followed by several short temperature flashes to 1250 °C. Sample and sample holder had been degassed before at 700 °C for several hours. This procedure routinely resulted in a (7 × 7) reconstructed surface showing flat areas at least 2000 Å wide. Although the germanium layer desolves into the bulk when the sample is again flashed to 1250 °C, a new substrate sample was prepared for each Ge deposition to minimize contamination effects. The substrates showing the

<sup>1</sup> Present address: Arbeitsgruppe für Halbleiterphysik, Hausvogteiplatz 5/7, O-1086 Berlin, Germany.

boron segregated ( $\sqrt{3} \times \sqrt{3}$ )R30° were prepared in the same manner, but by using 0.002  $\Omega \cdot \text{cm}$  boron-doped Si(111) wafers instead. Germanium was deposited with a deposition rate of  $\sim 1$  ML in 50 s from a graphite tube which was heated by electron bombardment (1 ML =  $7.84 \times 10^{14}$  atoms/cm<sup>2</sup>). Before supplying it with the Ge evaporation material, the graphite tube was, carefully degassed at 1800 °C. An absolute calibration of the incoming Ge flux was achieved by measuring the fraction of the surface covered with ordered Ge islands in the submonolayer range for a given deposition time. The deposition was always done with the substrate at the temperature indicated, then the sample was quenched to room temperature and transferred to the STM after  $\sim 1$  h. All STM images shown here (except fig. 3) are obtained with the sample at positive bias voltage (electrons tunneling into empty surface states of the sample) and a tunneling current of  $\sim 1$  nA. The images are either displayed in a top view greyscale representation or as a pseudo three-dimensional perspective image.

### 3. Results

#### 3.1. Nucleation and strained-layers growth

Fig. 1 shows the result of a Ge deposition with the substrate kept at room temperature. As expected, we do not find an ordered overlayer but irregular clusters. The substrate (7×7) reconstruction is unaffected in agreement with the literature [3]. Although the individual Ge clusters have random shapes, they form a nearly ordered array on the substrate (7×7) reconstruction. They almost never cover a (7×7) cornerhole. In most cases there are two Ge clusters in each (7×7) unit cell; one in each sub-triangle. No preference for clustering on the faulted half of the (7×7) unit cell as found for Pd<sub>2</sub>Si [4] and silver [5] is observed. Exactly the same nucleation behaviour is also observed for the growth of Si on Si(111)-(7×7) [6]. There it could be shown that the atoms impinging on the surface at first bond to the

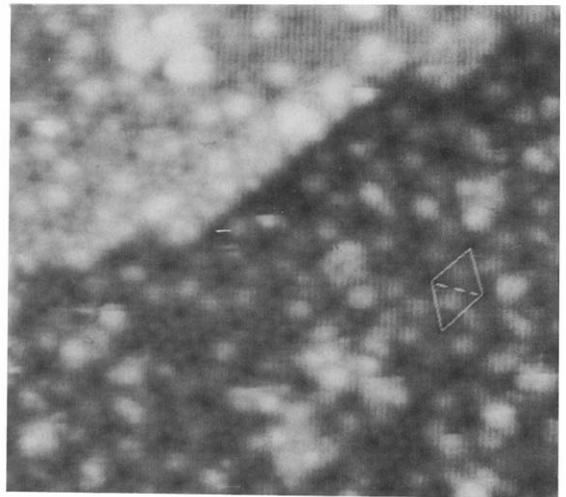


Fig. 1. 0.4 ML GE deposited at room temperature; the image shows an area of 270 Å×240 Å. A (7×7) unit cell is indicated. It is visible that the step edge in the upper left part of the image has no influence on the distribution of the Ge clusters.

rest-atoms in the substrate (7×7) reconstruction. This gives a natural explanation for the clustering of Si and Ge in the middle of the two sub-triangles of the substrate reconstruction. Each triangle of the (7×7) unit cell has three rest-atoms and, if these sites are occupied first, a base is formed for two clusters separated by the boundary between faulted and unfaulted half where the atoms form dimer bonds. In this region there are no dangling bonds to adsorb to, and the coalescence of clusters is inhibited (at least in the early stage of nucleation). Despite of the low deposition temperature the arriving atoms must have a certain mobility high enough for forming clusters at these special sites but not sufficient for agglomeration at step edges as can be seen in the upper left of fig. 1. Therefore we can estimate an average diffusion length at room temperature in the order of the size of half a (7×7) unit cell ( $\sim 15$  Å).

The growth of ordered epitaxial Ge layers was achieved when the substrate temperature during deposition was above 350 °C. From literature it is known that these Ge layers are laterally compressed to match the silicon lattice constant [1]. Fig. 2a shows the result of 0.4 ML Ge deposition at 450 °C. A triangular shaped island has been formed. There are three preferential directions of

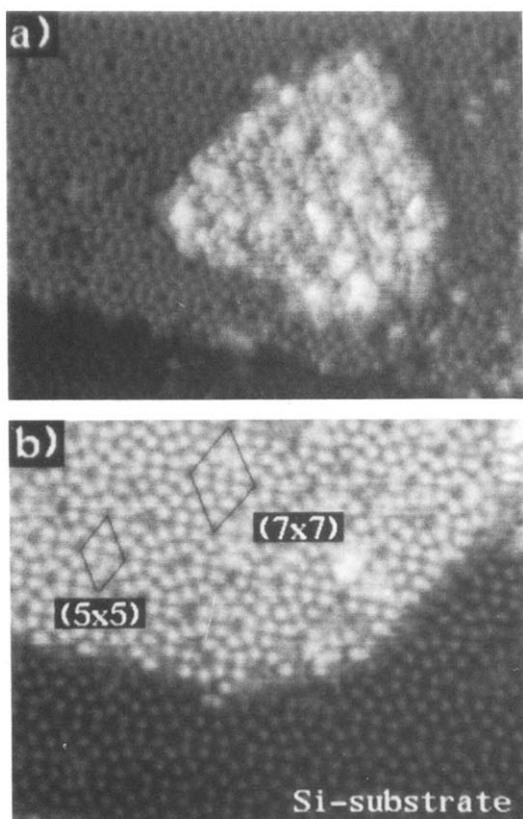


Fig. 2. Epitaxial Ge islands grown at elevated substrate temperature showing silicon-like reconstructions: (a) Triangular shaped island with  $(7 \times 7)$  reconstruction on top. (b) Fraction of a bigger epitaxial island; a  $(5 \times 5)$  and a  $(7 \times 7)$  unit cell are indicated schematically.

growth, reflecting the threefold symmetry of the Si(111) surface. If we determine the orientation of the epi-islands on the substrate, we see that the growth in  $[\bar{1}\bar{1}2]$  direction is preferred. The growth occurs always in complete bilayers; we never observed islands with a smaller step height than 3.3 Å. The surface of the island is reconstructed but the reconstruction is not  $c(2 \times 8)$  as one would expect for germanium. Instead we find a Si-like  $(7 \times 7)$  reconstruction on top of the germanium island as has already been found in electron diffraction [12,24]. In fig. 2b a fraction of a bigger island grown at 480 °C is shown. This island exhibits a mixture of  $(7 \times 7)$  and  $(5 \times 5)$  reconstructed surface areas. Tunneling spectroscopy performed and images obtained at different bias

voltages (fig. 3) are in accordance with the usual dimer-adatom-stacking fault (DAS) model [7] for these Ge reconstructions. Becker et al. [8] have shown the same to hold for the  $(5 \times 5)$  reconstruction found on Ge/Si alloys. Generally it is believed that the strain in the germanium layer induced by the 4% misfit to the substrate is responsible for the formation of the  $(5 \times 5)$  reconstruction. From the minimum fraction of Ge in Ge/Si alloys to form a  $(5 \times 5)$ , a lower limit for the necessary elastic strain has been calculated [9]. On the other hand, a  $(5 \times 5)$  reconstruction is also present as a metastable structure in the homoepitaxy of Si on Si(111)-(7×7) [6,10]. Hence, the stress in the adlayer cannot be the only reason for the formation of the  $(5 \times 5)$  reconstruction.

Although the same superstructures are present on epitaxial layers of silicon and germanium on Si(111)-(7×7) the relative fractions are different for both systems. Whereas the Si on Si system displays predominantly  $(7 \times 7)$  reconstructed regions, the  $(5 \times 5)$  reconstruction is preferred for the Ge on Si system. When the Ge coverage exceeds 2 ML the epilayer is nearly exclusively covered by a  $(5 \times 5)$  reconstruction (fig. 3). Different translational domains of the  $(5 \times 5)$  are visible indicating

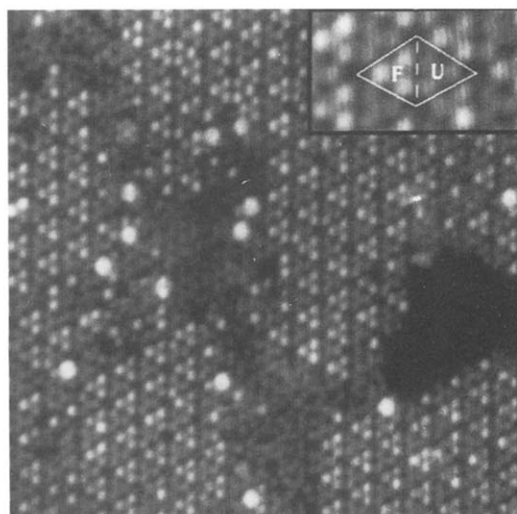


Fig. 3. Strictly  $(5 \times 5)$  reconstructed layer of 4 ML germanium deposited at 420 °C. The bias voltage at the sample is  $-1.7$  V (tunneling from filled states of the sample). The insert magnifies a  $(5 \times 5)$  unit cell showing the electronic asymmetry between faulted and unfaulted half of the  $(5 \times 5)$  unit cell.

that this layer was formed by the coalescence of independently nucleated islands. Fig. 3 depicts an image of the filled states of the Ge surface showing the electronic difference between faulted and unfaulted half of the  $(5 \times 5)$  DAS unit cell (see insert of fig. 3). Tunneling spectroscopy shows that the electronic structure of the Ge(111) DAS structures within the detection limit is identical to the Si(111)-(7×7). Indeed, for the growth at step edges it was often impossible to determine the exact boundary between silicon and germanium.

Bulk diffusion coefficients predict negligible interdiffusion below 600 °C [1]. Auger-spectroscopy results [3] show for a temperature up to 520 °C an exponential decrease in the Si(LVV) signal with increasing Ge covering up to 3 ML, indicating no alloying in agreement with RBS results [12]. Therefore it is reasonable to assume that also no intermixing of Ge and Si takes place at the lateral interface.

### 3.2. Influence of defects

It is always an important question how defects present at the substrate surface influence the nucleation and growth behaviour. Especially the presence of sites providing a higher nucleation probability are of interest because they lead to inhomogeneities in the local surface coverage. This is the case in fig. 4a. The Ge islands are located preferentially along certain lines on the surface. Fig. 4b zooms into a region around such a line of higher island density. A line is drawn through the cornerholes of the substrate  $(7 \times 7)$  reconstruction on the left hand side of the Ge island. After the line has crossed the Ge island it does not match with the cornerhole position any more indicating that underneath the epitaxial island there is a translational domain boundary separating different  $(7 \times 7)$  domains. The higher number of broken bonds or the stress field along such a boundary seems to be responsible for the preferred nucleation. The islands in fig. 4 have formed a nearly closed line and one can easily imagine that, once the line has closed, it behaves identically to a step edge with respect to the nucleation behaviour. That means it will attract diffusing Ge atoms and suppress any nucleation close by (see fig. 5). This

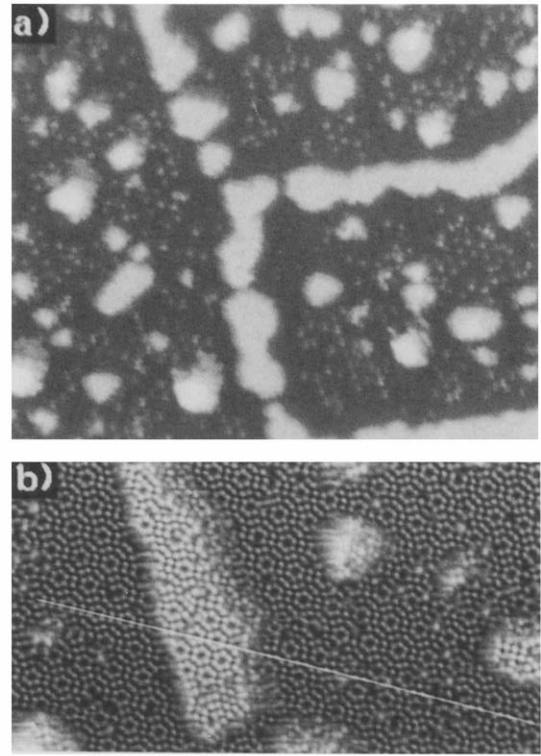


Fig. 4. Preferred nucleation at domain boundaries of the  $(7 \times 7)$  superstructure of the substrate: (a) Large area scan ( $2400 \text{ \AA} \times 2000 \text{ \AA}$ ). (b) Atomic scale details; the line through the cornerholes of the substrate  $(7 \times 7)$  shows the displacement of the domains underneath the Ge island.

leads to strong variations in the Ge coverage even in absolutely flat regions of the substrate which we often observed. The preferential nucleation at  $(7 \times 7)$  domain boundaries is another example for the similarity between the heteroepitaxy of germanium and the homoepitaxy on Si on Si(111)-(7×7), where exactly the same behaviour has been found [6].

A second defect always present on the substrate are monatomic steps. Fig. 5 shows the influence of these steps on the nucleation behaviour. Around the step edge visible in the lower right corner of fig. 5a, a region of the substrate is depleted of separately nucleated islands. Higher resolved images show that instead the step edge has locally roughened indicating that there germanium has attached to the step edge. In fig. 5b the effect of 4 ML Ge deposition onto a substrate having a ran-

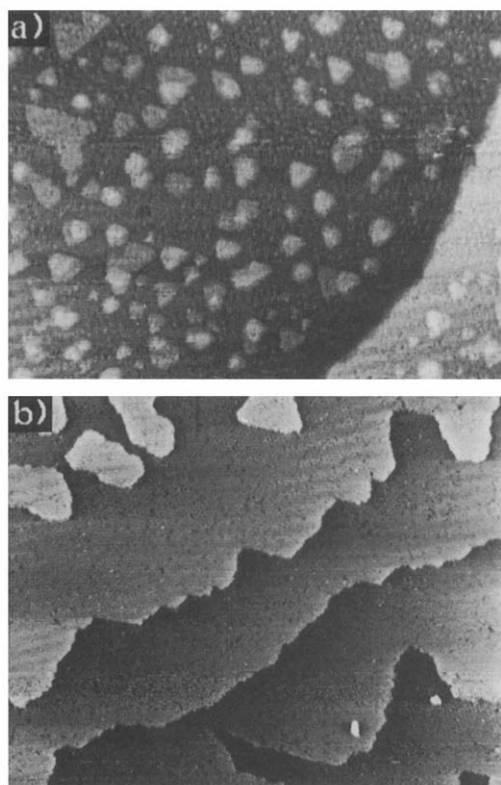


Fig. 5. Influence of substrate steps: (a) Area of  $1500 \text{ \AA} \times 1000 \text{ \AA}$ . 0.4 ML Ge deposited at  $420^\circ \text{C}$ . The depletion of islands in the neighbourhood of a step edge is visible in the lower right corner. (b) Area of  $3500 \text{ \AA} \times 2500 \text{ \AA}$ ; 4 ML germanium deposited at  $500^\circ \text{C}$  onto a stepped substrate.

dom miscut of  $0.5^\circ$  is shown. The deposition temperature was  $80^\circ \text{C}$  higher than in fig. 5a and the growth by step propagation is the dominant process. The initially nearly straight step edges start the meander. This is understandable because the macroscopic direction of the substrate steps is not along one of the directions which are preferred in Ge growth and we find therefore a kind of “one-dimensional faceting” along the step edge. Independently nucleated islands are only present on the large terrace in the upper left of fig. 5b. Each step edge has a certain influence range where it attracts all Ge material. We can estimate this effective diffusion length to be  $120 \text{ \AA}$  for the  $420^\circ \text{C}$  deposition and  $800 \text{ \AA}$  for the  $500^\circ \text{C}$  deposition symmetrically to both sides of the step edge. When the local step separation is smaller

than this value, islanding is completely suppressed (see fig. 5b).

To summarize the results for the submonolayer regime, we can state that the behaviour of the Ge on Si(111) system is nearly a perfect copy of the system Si on Si(111). Not only is the lateral lattice constant of the germanium compressed to match the silicon constant, but the germanium also adopts the silicon surface reconstructions. Differences are only found for the relative fractions of  $(5 \times 5)$  and  $(7 \times 7)$ , which finally leads around 4 ML Ge coverage to an exclusively  $(5 \times 5)$  reconstructed layer.

### 3.3. Nucleation on the boron segregated $(\sqrt{3} \times \sqrt{3})R30^\circ$ surface

One question arising in the pseudomorphic growth regime is whether the presence of the  $(7 \times 7)$  reconstruction on the substrate is necessary to nucleate the Si-like reconstructions in the Ge epilayer. A simple way to prevent the Si(111) surface from forming the  $(7 \times 7)$  reconstruction is to use a highly boron doped Si sample as substrate [13–16]. Upon annealing, boron segregates to the surface and a boron stabilized  $(\sqrt{3} \times \sqrt{3})R30^\circ$  reconstruction is formed (fig. 6a). Two different kinds of protrusions are visible at positive sample bias: “dark” and “bright” atom sites arranged in small domains of a  $(\sqrt{3} \times \sqrt{3})R30^\circ$  lattice. On substrates with higher boron concentration the number of “dark” atom sites is increased [15]; therefore, these atoms seem to be associated with the presence of boron close by. Different models are offered in the literature for this surface. The “dark” and “bright” atoms are either interpreted as boron and silicon atoms located at  $T_4$  adatom sites on top of the surface [13]. In a different explanation the boron atoms are placed underneath the surface in a five-fold coordinated  $B_5$  site [14–16]. In the latter case all atoms visible in the STM image are suggested to be silicon atoms, the “dark” ones with a boron atom located underneath them.

Such a surface is used as a substrate for the Ge growth at  $420^\circ \text{C}$  shown in fig. 6b. Three terraces separated by monatomic steps are visible on which epitaxial Ge islands have nucleated. Although the

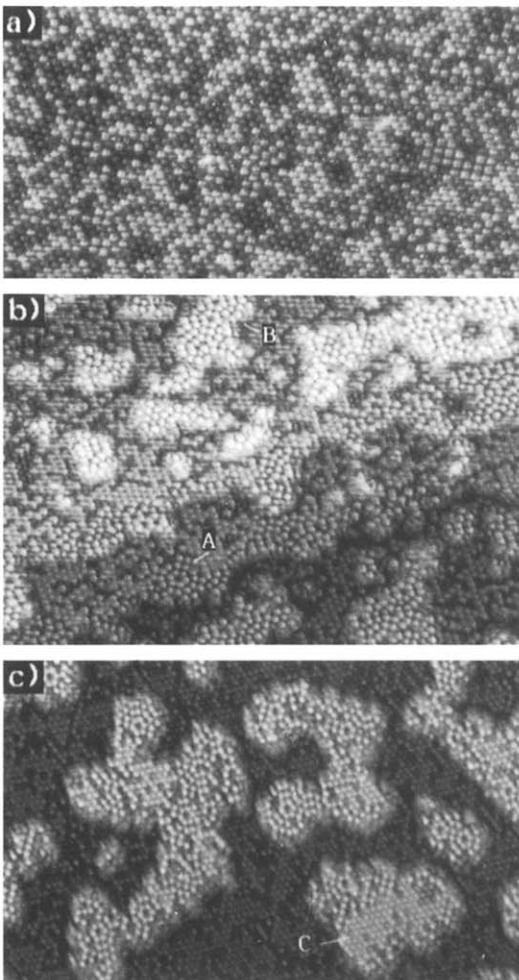


Fig. 6. (a) Boron segregated Si(111)/B( $\sqrt{3} \times \sqrt{3}$ )R30°. (b) 0.6 ML Ge deposited at 420°C onto this surface. The image shows three terraces separated by monatomic steps. Marker (A) and (B) indicate Ge-(5×5) structures at a step edge and on an epitaxial island. (c) Same surface as in (b); annealed to 480°C. Marker (C) points to an island where the boron has already segregated into the island.

substrate still shows the boron stabilized ( $\sqrt{3} \times \sqrt{3}$ )R30° reconstruction, the islands have DAS-like reconstructions on top (see position marked B in fig. 6b) which are in most cases small domains of (5×5) reconstruction. In more disordered looking regions on the islands the reconstructions consist mostly of small domains of (2×2)-arranged adatom structures. Also at the step edges the growth of DAS structures is visible (position A). Due to these different types of re-

construction we can distinguish between the substrate and the epi-material and determine exactly the interface between the original Si-substrate step and the epitaxially grown germanium. Within the substrate layer the Ge reconstructions of the kind known from pure Si substrates are only present at step edges indicating that at the low deposition temperature used (420°C) no intermixing between silicon and germanium occurs. At this temperature there is also no indication for any boron diffusion through the Ge layer because no  $\sqrt{3}$  structures indicating the presence of boron (see next paragraph) are found on the epi-islands or in the germanium covered regions at step edges.

The occurrence of the DAS-like structures in the epitaxial germanium also in the case of a non-DAS reconstructed substrate is a clear hint for the substrate reconstruction to be of only minor importance for the appearance of the DAS structures.

The morphology of islands is quite different on the boron segregated Si surface compared to epitaxy on the clean Si(111)-(7×7) surface. The shape of islands is more irregular than on the (7×7) substrate at comparable temperature. Only islands showing a perfect (5×5) reconstruction on top have a triangular shape.

If the surface as prepared in fig. 6b is annealed at 480°C for 15 min, the image changes to the one shown in fig. 6c. Besides the coarsening of islands due to the higher annealing temperatures as on the clean substrate on some islands the reconstruction has partially changed to a ( $\sqrt{3} \times \sqrt{3}$ )R30° similar to the one on the substrate. (See C in fig. 6c.) A temperature of 480°C seems to be sufficient for the boron to diffuse through the Ge islands and to introduce a  $\sqrt{3}$  reconstruction, too. Therefore it is impossible to grow islands showing long range ordered DAS structures on this surface because at the higher temperature required, the boron destroys the DAS reconstructions. For further details of the growth on these structures see ref. [17].

### 3.4. Islanding

If the Ge coverage exceeds 4 ML, the formation of three-dimensional islands begins. Fig. 7 shows a

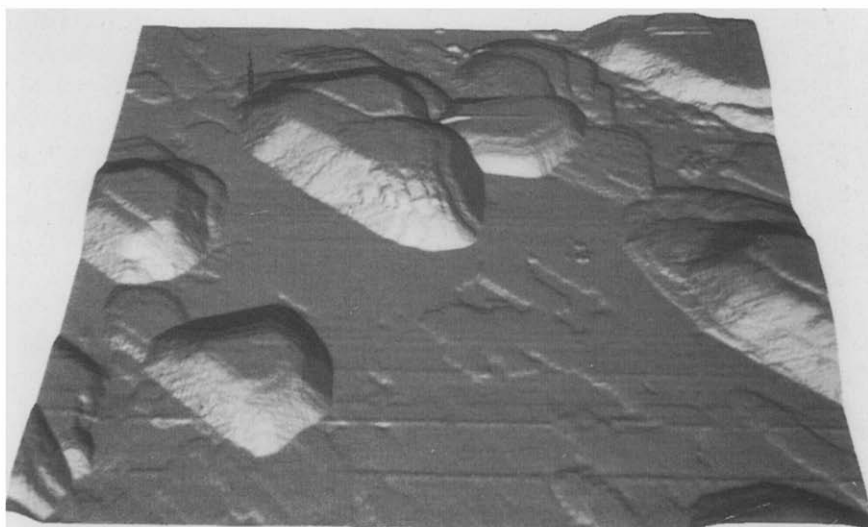


Fig. 7. Perspective view of a  $3000 \text{ \AA} \times 2000 \text{ \AA}$  area after 9 ML Ge deposition at  $420^\circ \text{C}$ . The 3D islands have a height distribution ranging from 50 to 100  $\text{\AA}$ .

perspective view of a  $3000 \text{ \AA} \times 2000 \text{ \AA}$  area after 9 ML Ge deposition at  $420^\circ \text{C}$ . Again it confirms that germanium grows in the SK mode on Si(111). Usually in 3D rendered STM images the  $z$ -scale is enlarged by a factor between 10 and 100 to show the very small variations in height. In fig. 7 the scale factor is the same in  $x$ ,  $y$  and  $z$ -direction, to show the correct proportions. Despite of the low coverage, the 3D islands already display a height distribution ranging from 50 to 100  $\text{\AA}$ . In between the 3D islands, we still find perfectly flat regions with monatomic steps. (Such a step edge can be seen in the middle of fig. 7.) Higher resolved images of these regions show, that they are still covered by a  $(5 \times 5)$  reconstruction. The transition from layer-by-layer growth up to 4 ML to islanding is abrupt, if the coverage exceeds 4 ML; no intermediate structures as observed for Ge growth on the Si(100) surface [18] have been found.

The 3D islands visible in fig. 7 have lateral dimensions from 300 to 1000  $\text{\AA}$ . We did not observe any preferential nucleation at step edges or other defects. The islands predominantly have a triangular shape and show ordered facets at the side and on top. The top facet is of course a (111). Especially on the smaller islands this facet often covers only a small fraction of the island surface.

(See e.g. the islands in the lower left corner of fig. 7.) When the islands grow bigger at higher Ge coverage, the fraction of the (111) facet usually increases, but we never found an island without (111) facet on top. The main facet making up the side walls of the islands is a (113) as determined by measuring the angle to the (111) plane and from the lateral orientation. STM images with atomic resolution on the (113) facet show, that they have a  $(1 \times 3)$  reconstruction, as observed by LEED on Si and Ge samples cut in the (113) plane [19].

If we compare the lattice constant of the  $(5 \times 5)$  in between the 3D islands and the spacing on the islands, we find that, within the uncertainty of STM measurements ( $\sim 1\text{--}2\%$ ), the islands have relaxed to the bulk germanium lattice constant. Accordingly, the top (111) facet of the 3D islands is reconstructed in the usual superstructures observed on bulk Ge(111) crystals [20,21]. Fig. 8 shows the top of the 3D island also grown at  $420^\circ \text{C}$  substrate temperature. The three major reconstructions present at the Ge(111) surface are indicated. The  $c(2 \times 8)$ , the structure usually observed with LEED on Ge(111), covers only  $\sim 40\text{--}50\%$  of the surface. The rest is covered by a mixture of small domains of  $(2 \times 2)$  and  $c(2 \times 4)$ .



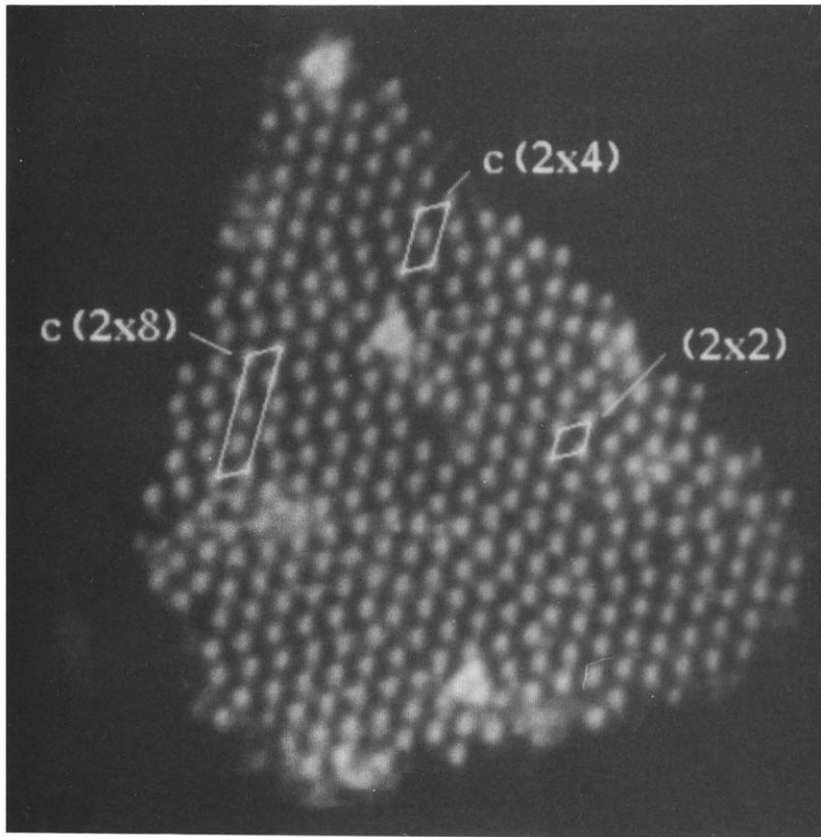


Fig. 8. Top of a 3D island showing the typical Ge reconstructions.

Higher deposition temperature generally results in a higher fraction of  $c(2 \times 8)$  indicating that this structure has the lowest energy. As we will see below, there is a limit for the development of ordered Ge reconstructions by annealing to higher temperature. It has been shown, that all these reconstructions are simple adatom arrangements with the adatoms sitting in  $T_4$  sites [20]. The  $c(2 \times 8)$  can be regarded as an alternating sequence of two translational  $(2 \times 2)$  domains. No subsurface stacking fault as in the Si-( $7 \times 7$ ) reconstruction seems to be involved [20]. At this deposition temperature ( $420^\circ\text{C}$ ) no DAS structures are present on the (111) facet of the 3D islands.

If the substrate temperature during deposition is raised to  $500^\circ\text{C}$ , the appearance of the top surface of the 3D islands changes drastically. In some regions the island surface still shows the

typical Ge-type reconstructions ( $(c(2 \times 8), (2 \times 2), c(2 \times 4))$ ), but the majority of the surface is again covered by a  $(7 \times 7)$  reconstruction. At even higher deposition temperature the island surface is completely  $(7 \times 7)$  reconstruction. LEED [24] and RHEED investigations [9] show the same behaviour, but the result was interpreted differently in these two studies. The authors of ref. [24] related the reappearance of the  $(7 \times 7)$  to residual compressive strain in the Ge layer, whereas in ref. [9] Si segregation to the surface was proposed. The temperature dependence of the effect (Ge-like structures for deposition below  $450^\circ\text{C}$  and  $(7 \times 7)$  above  $450^\circ\text{C}$ ) seems to be consistent with both explanations. A higher substrate temperature during deposition could favour segregation to the surface but also induce strain due to the difference in linear thermal expansion between germanium and silicon. We performed tunneling spectroscopy



to clarify this point. Indeed, there are differences between areas showing  $(7 \times 7)$  and areas with  $c(2 \times 8)$  reconstruction. But from these data alone it is impossible to distinguish between Ge and Si in the surface layer.

### 3.5. Bulk defects in the SK islands

For Ge epitaxy on the Si(100)-(2 × 1) it was proposed, basing on TEM results [22], that the 3D islands are initially dislocation-free, and the mismatch is accommodated by elastic deformation in the substrate in the vicinity of the islands. If the same holds for the Si(111) surface, we should not expect to find a high density of bulk defects in the

3D islands. Another problem related to STM is that we will see such defects only emerging from the bulk, if they intersect the surface. Therefore, with STM alone it is impossible to make a quantitative analysis of the defect density in the islands. In this section we just want to present two typical bulk defects often found. Fig. 9a shows a fraction of an island, 3000 Å in diameter, grown at 450 °C with a macroscopic coverage of 40 ML. As already noted, at higher Ge-coverage the ratio of the lateral to the vertical dimensions of the islands increases; i.e. the top (111) facet grows at the expense of the other facets. Several monatomic steps of the Ge(111) plane are visible in the lower right of fig. 9a, before a (113) facet begins going

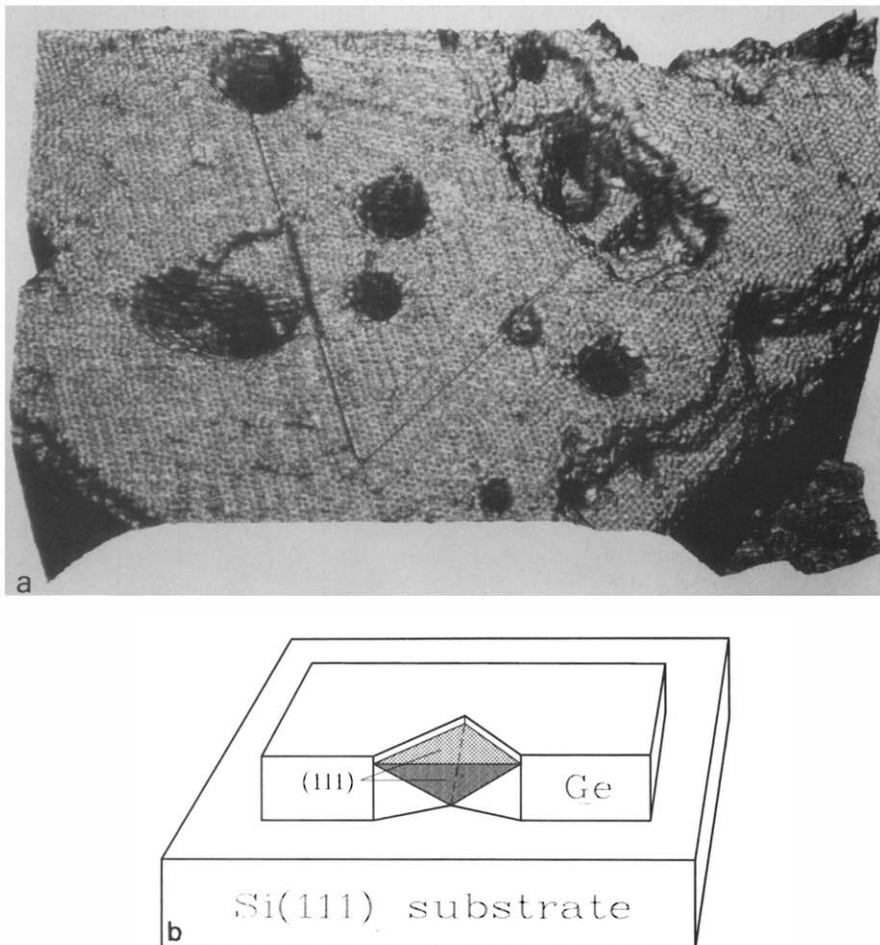


Fig. 9. (a) Perspective view ( $1200 \text{ \AA} \times 750 \text{ \AA}$ ) of a fraction of a 3D island containing a stacking fault tetrahedron. The hole at the upper right corner of the triangle allows a view at lower layers of the defect. (b) Schematic of a stacking fault tetrahedron.

down to the SK layer in between the 3D islands. This layer itself could not be imaged because, due to the increasing roughness of the surface, multiple tip imaging became a serious problem. (The macroscopically “blunt” tip did not fit in between the islands.) A 500 Å wide triangular structure and several holes are visible on top of the island. The inner part of the triangle is  $\sim 1.1$  Å lower than the outer part. This non-integral step height (the bilayer distance of the Ge(111) surface is 3.3 Å) indicates, that here a bulk defect is involved. A grid superimposed on a region around this step edge shows that there is also a lateral shift between inner and outer part of the triangle of  $1/6$   $[\bar{1}\bar{1}2]$ . Taking into account these two pieces of information, and looking into the literature, one finds that this structure can be identified as a *stacking fault tetrahedron* (fig. 9b), a bulk defect found in fcc and diamond lattices [23]. The triangle we see at the surface is one of the four (111) surfaces of a tetrahedron shaped crystallite within the crystal. A fault in the stacking sequence of the (111) planes occurs at each surface of this tetrahedron. There are no Ge atoms in a non-ideal configuration on these planes, broken bonds exist only at the edges of the tetrahedron. If we model such a defect, we get the vertical and the lateral shift in the surface lattices we determined from fig. 9a. One apex of the tetrahedron is usually

believed to be at the interface. Hence, one can estimate the local height of this 3D island to be  $\sim 400$  Å. The big hole at the upper right corner of the triangle in fig. 9a enables us to have a look at lower layers of the island, and proves the model mentioned above for the defect right. It is clearly visible that the triangle is continued on the lower layers. Close inspection also shows that the 1.1 Å step edge moves inward on lower layers as is expected from the model.

In fig. 10 the defect is shown we found most frequently. It contains a 1.1 Å step edge similar to the one involved in the above defect. This step line is terminated on both sides by a screw dislocation-like structure. This defect can be identified as a stacking fault in a (111) plane penetrating into the bulk and being enclosed by partial dislocations. The Burgers vectors of the two partial dislocations add to a vector parallel to the surface, so that an edge dislocation results, which splits into the two partial dislocations. The distance of the partial dislocations was found to vary between 100 Å and over 1000 Å. In the neighbourhood of bulk defects holes in the epilayer were often found. (See fig. 9 and fig. 10.) Most of these holes were deeper than the STM tip could explore; i.e. at least 5–10 layers. Especially the partial dislocations as in fig. 10 were always accompanied by holes with a typical diameter of 50–100 Å. A more detailed analy-

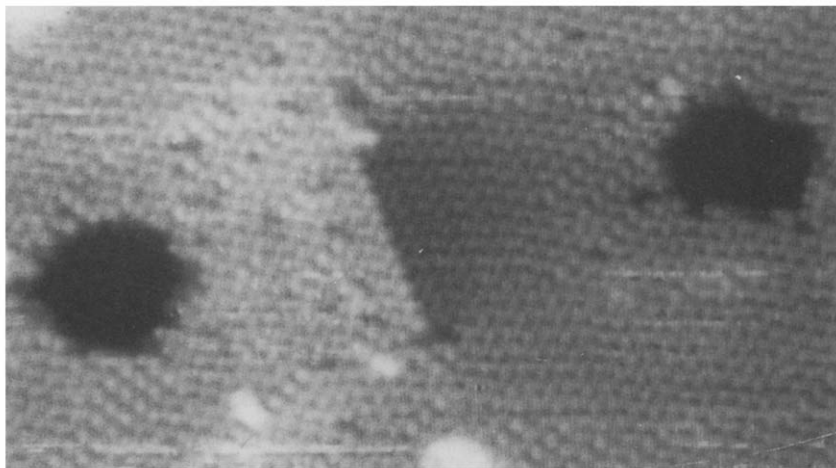


Fig. 10. Stacking fault on a (111) plane going down into the bulk bounded by partial dislocations. The Ge island was grown at 450 °C.

sis of the defects found on the 3D islands will be given elsewhere.

In summary, the different stages of epitaxial growth of germanium on Si(111) surfaces were imaged showing that mesoscopic features like the homogeneity of the local Ge coverage on the substrate are strongly influenced by typical atomic scale defects of the substrate. The reconstructions of the epilayer were shown to be inherent properties of species grown under stress as there is no dependence on the initial substrate reconstruction.

The reason for the reappearance of the (7 × 7) reconstruction on 3D islands at higher deposition temperature remains an open question for further experiments.

### Acknowledgements

The investigation has been supported by the Volkswagen Stiftung. The silicon crystals have been kindly provided by Wacker Chemitronic, Burghausen (Germany).

### References

- [1] G.J. Fisanick, H.-J. Gossmann and P. Kuo, *Mat. Res. Soc. Symp. Proc.* 102 (1988) 25.
- [2] J.E. Demuth, R.J. Hamers, R.M. Tromp and M.E. Welland, *J. Vac. Sci. Technol. A* 4 (1986) 1320.
- [3] H.-J. Gossmann, L.C. Feldman and W.M. Gibson, *Surf. Sci.* 155 (1985) 413.
- [4] U.K. Köhler, J.E. Demuth and R.J. Hamers, *Phys. Rev. Lett.* 60 (1988) 2499.
- [5] St. Tosch and H. Neddermeyer, *Phys. Rev. Lett.* 61 (1988) 349.
- [6] U. Köhler, J.E. Demuth and R.J. Hamers, *J. Vac. Sci. Technol. A* 7 (1989) 2860.
- [7] K. Takayanagi, Y. Tanishiro, S. Takahashi and M. Takahashi, *Surf. Sci.* 164 (1985) 367.
- [8] R.S. Becker, J.A. Golovchenko and B.S. Swartzentruber, *Phys. Rev. B* 32 (1985) 8455.
- [9] M.A. Lamin, O.P. Pchelyakov, L.V. Sokolov, S.I. Stenin and A.I. Toropov, *Surf. Sci.* 207 (1989) 418.
- [10] M. Horn von Hoegen, J. Falta and M. Henzler, *Thin Solid Films* 183 (1989) 213.
- [11] G.L. Mc Vay and A.R. DuCharme, *J. Appl. Phys.* 44 (1973) 1409.
- [12] P.M.J. Marée, K. Nakagawa, F.M. Mulders, J.F. van der Veen and K.L. Kavanagh, *Surf. Sci.* 191 (1987) 305.
- [13] I.-W. Lyo, E. Kaxiras and Ph. Avouris, *Phys. Rev. Lett.* 63 (1989) 1261.
- [14] P. Bedrossian, K. Mortensen, D.M. Chen and J.A. Golovchenko, *Phys. Rev. B* 41 (1990) 7545.
- [15] P. Bedrossian, R.D. Meade, K. Mortensen, D.M. Chen, J.A. Golovchenko and D. Vanderbilt, *Phys. Rev. Lett.* 63 (1989) 1257.
- [16] R.L. Hendrick, I.K. Robinson, E. Vlieg and L.C. Feldman, *Phys. Rev. Lett.* 63 (1989) 1253.
- [17] U. Köhler, B. Müller, O. Jusko and G. Pietsch, in preparation.
- [18] Y.-W. Mo, D.E. Savage, B.S. Swartzentruber and M.G. Lagally, *Phys. Rev. Lett.* 65 (1990) 1020.
- [19] U. Myler and K. Jakobi, *Surf. Sci.* 220 (1989) 353.
- [20] R.S. Becker, B.S. Swartzentruber and J.S. Vickers, *J. Vac. Sci. Technol. A* 6 (1988) 472.
- [21] R.S. Becker, J.A. Golovchenko and B.S. Swartzentruber, *Phys. Rev. Lett.* 54 (1985) 2678.
- [22] D.J. Ealesham and M. Cerullo, *Phys. Rev. Lett.* 64 (1990) 1943.
- [23] R.H. Finch and H.J. Queisser, *J. Appl. Phys.* 34 (1963) 406.
- [24] H.-J. Gossmann, J.C. Bean, L.C. Feldman, E.G. McRae and I.K. Robinson, *Phys. Rev. Lett.* 55 (1985) 1106.